Journal of Hand Surgery Global Online 3 (2021) 240–244

Contents lists available at ScienceDirect

Journal of Hand Surgery Global Online

journal homepage: www.JHSGO.org

Original Research

Long-term Evaluation Using Finite Element Analysis of Bone Atrophy Changes after Locking Plate Fixation of Forearm Diaphyseal Fracture

Tetsuya Hirashima, [*] Yusuke Matsuura, MD, PhD, [†] Takane Suzuki, MD, PhD, [‡] Tomoyo Akasaka, MD, PhD, [§] Aya Kanazuka, MD, PhD, [†] Seiji Ohtori, MD, PhD [†]

[*] School of Medicine, Chiba University, Chiba City, Japan
[†] Department of Orthopaedic Surgery, Graduate School of Medicine, Chiba University, Chiba City, Japan
[‡] Department of Bioenvironmental Medicine, Graduate School of Medicine, Chiba University, Chiba City, Japan
[§] Department of Rehabilitation Medicine, Graduate School of Medicine, Chiba University, Chiba City, Japan

ARTICLE INFO

Article history:
Received for publication December 1, 2020
Accepted in revised form May 26, 2021
Available online June 14, 2021

Key words:
Bone mineral density
Bone strength
Finite element analysis
Forearm fracture
Plate fixation

Purpose: To determine the optimal timing of plate removal in patients with forearm diaphyseal fractures fixed with a locking plate via the analysis of bone atrophy over time.
Methods: The study subject was a 56-year-old man. Computed tomography was performed at 0.5, 1, 1.5, 2, 3, 4, and 5 years after plate fixation. Finite element analysis was performed to measure the fracture load of the radius and ulna. The fracture loads of the affected and healthy sides were compared, and their ratio was calculated by dividing the value of the affected side by that of the healthy side at each time point.
Results: The strength of the radius and ulna was 40.9% and 29.3%, respectively, on the healthy side at 1 year after surgery. The fracture load increased from the second to the third postoperative year; the strength of the radius and ulna was 62.2% and 37.3%, respectively, on the healthy side after the third year. However, after the third year, the fracture load declined and reached 38.8% and 18.9% for the radius and ulna, respectively, on the healthy side by the fifth postoperative year.
Conclusions: The long-term fixation of forearm diaphyseal fractures using a locking plate leads to progressive bone atrophy. Future bone atrophy during long-term locking plate fixation without removal should be monitored.
Type of study/level of evidence: Therapeutic IV.

Copyright © 2021, THE AUTHORS. Published by Elsevier Inc. on behalf of The American Society for Surgery of the Hand. This is an open access article under the CC BY-NC-ND license (http://creativecommons.org/licenses/by-nc-nd/4.0/).

Open reduction and internal fixation with a plate is widely used for treating forearm diaphyseal fractures in adults, and good outcomes have been reported.[1] Internal fixation with a nonlocking plate may be used to treat forearm diaphyseal fractures, or alternatively, osteoporotic and highly comminuted fractures may be treated with a locking plate, with good results.[2] However, plate removal is associated with various complications, the most serious of which is a refracture.[3]

Local bone atrophy has been suggested to contribute to the occurrence of a refracture, with impaired blood flow after plate fixation considered as the underlying mechanism.[4,5] In a study using sheep, Klaue et al[6] described that cortical porosis observed in the vicinity of the plate was mainly a result of periosteal blood supply impairment due to periosteal stripping and subperiosteal plate application rather than due to the "unloading" of the bone by the plate. Conversely, previous biomechanical studies have demonstrated the advantages of stabilization using locking screws over nonlocking screws.[7] The use of large plates fixed to small bones (eg, in rabbits) has been reported to result in bone atrophy, whereas the use of plates with varying flexibility (eg, carbon fiber) on large bones has been shown to lead to a nonunion because of strain.[8] Therefore, local bone atrophy may also be affected by the mechanical environment to which the bone is subjected.

Declaration of interests: No benefits in any form have been received or will be received related directly or indirectly to the subject of this article.

Corresponding author: Yusuke Matsuura, MD, PhD, Department of Orthopaedic Surgery, Graduate School of Medicine, Chiba University, 1-8-1 Inohana, Chuo-ku, Chiba, 260-8670, Japan
E-mail address: y-m-1211@khaki.plala.or.jp (Y. Matsuura).

https://doi.org/10.1016/j.jhsg.2021.05.013
2589-5141/Copyright © 2021, THE AUTHORS. Published by Elsevier Inc. on behalf of The American Society for Surgery of the Hand. This is an open access article under the CC BY-NC-ND license (http://creativecommons.org/licenses/by-nc-nd/4.0/).

Figure 1. Plain X-ray images. **A** Preoperative X-ray image showing a metaphyseal fracture of the forearm. **B** Postoperative X-ray image following open reduction and internal fixation using a locking plate. **C** Preoperative X-ray image showing a distal humerus fracture. **D** Postoperative X-ray image following open reduction and internal fixation using locking plates.

As a noninvasive method of predicting fracture strength, patient-specific computed tomography (CT) or finite element analysis (FEA), which uses local bone density distribution converted from CT Hounsfield unit (HU) values to create a model, has been used by many researchers.[9–14] Matsuura et al[15] conducted a validation study of the forearm diaphysis using fresh-frozen cadavers. In a study on patient-specific CT or FEA, it was reported that 5 years after surgery, patients who had undergone locking plate fixation for forearm diaphyseal fractures had significant bone atrophy compared with patients who had undergone conventional plate fixation. Stress shielding due to the angular stability of the locking plate was reported as the cause of bone atrophy.[16] However, no reports on bone atrophy changes over time after locking plate fixation have been published, and the postoperative course of bone atrophy remains unclear.

The present study aimed to evaluate bone atrophy changes using patient-specific CT or FEA after the fixation of a forearm diaphyseal fracture using a lag screw and locking plate.

Materials and Methods

Study subject

The regional medical ethics committee of our hospital approved the study. We recruited a 54-year-old healthy man for the present study. He worked as a barber and was right-handed, with no pre-existing muscle weaknesses. He had a right humeral condyle open fracture (Arbeitsgemeinschaft Osteosynthese fragen classification [AO] 13A3.3) and right forearm diaphyseal closed fracture (AO 2R2B2, 2U2B2) after falling from a stepladder (Figs. 1A, 2A). Internal fixation was performed 11 days after the injury for all the fractures using a 3.5-mm locking compression posterolateral distal humerus plate with support (DePuy Synthes) and a 3.5-mm locking compression medial distal humerus plate (DePuy Synthes) for the distal humerus fracture and using a small-fragment locking compression plate (DePuy Synthes) for the forearm fractures (Fig. 1B). For the radius, after fixing the third bone fragment with a small cortical screw, this cortical screw was used as a lag screw over the plate to crimp the bone fragments, and the plate was fixed using 3 distal and 3 proximal locking screws for neutralization plating. For the ulna, after compression was obtained between the bone fragments using a cortical screw as a lag screw, the plate was further compressed to the bone using a cortical screw and fixed using 2 distal and 3 proximal locking screws for bridge plating.

Satisfactory fixation was achieved, and range of motion therapy was started without postoperative external fixation. The patient made full recovery and returned to his original job as a barber, without pain. The range of motion at 6 months after surgery was −5° of elbow extension, 140° of flexion, 80° of forearm

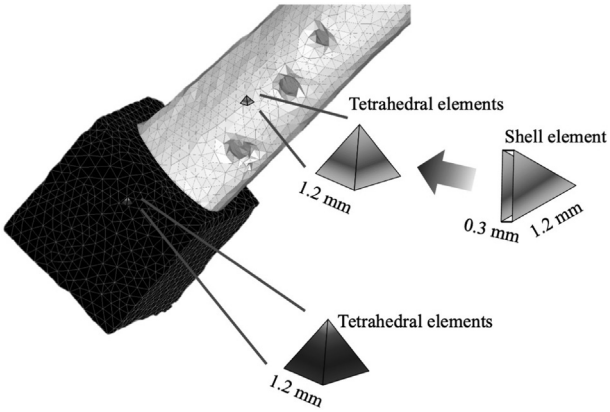

Figure 2. Diagram illustrating the selection of the area used for measuring BMD. We measured the average BMD of a 20-mm-long area of the forearm between the most distal proximal screw and the most recent distal screw of the plate.

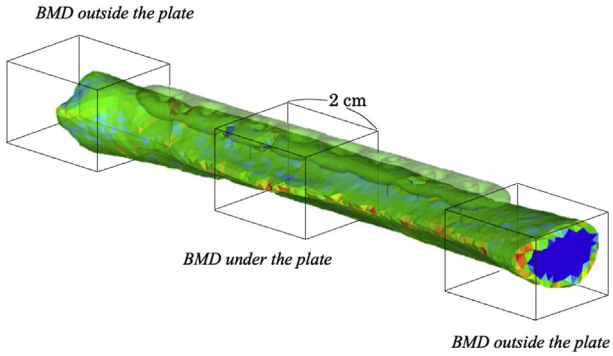

Figure 3. Diagram illustrating the creation of finite element models. A finite element model of bone and resin cement was constructed. Both the bone and resin cement were meshed with 1.2-mm primary mesh tetrahedral elements, and 0.3-mm thick shell elements were attached to the bone surface.

pronation, and 80° of supination, which was maintained until the final follow up. He did not take any osteoporosis medication.

The plate was not removed; therefore, patient consent was obtained, and plain X-ray and CT images of both the fractured and healthy contralateral forearms were taken at 0.5, 1, 1.5, 2, 3, 4, and 5 years after surgery using a Lightspeed VCT VISION scanner (GE Healthcare; a 64-row detector operated at 120 kV and 200 mA with a slice thickness of 0.65 mm and a pixel width of 0.5 mm).

Creating finite element models

We created a finite element model according to a previously validated protocol.[12] The CT Digital Imaging and COmmunications in Medicine data were imported into the Mechanical Finder FEA software (Computational Mechanics Research Center) to create a 3-dimensional (3D) model. The region of interest of the forearm was defined as the area in which the HU value was >1,000 HU. The range of interest of the plate and screws was set as the region where HU was ≥3,000 HU. The bone, resin cement, and the plate were meshed with linear tetrahedral elements with global edge lengths of 1.2, 1.2, and 0.3 mm, respectively. After generating the mesh, the plate area was removed using the software. The virtual thickness of the shell elements was set to 0.3 mm on the surface of the bone (Fig. 2). Surface elements were created to compensate for strength losses due to CT resolution effects.

Heterogeneous bone properties were assigned by defining the mechanical properties of each element based on the HU of the pixels occupying a common volume in 3D space, as per Equations 1 and 2:

Equation 1: Ash density (g/cm^3) = (HU + 1.4246) × 0.001/1.058 (HU value > −1)

Equation 2: Ash density (g/cm^3) = 0.0 (HU value ≤ −1)

To prevent metal artifacts, ash densities of >2.0 g/cm^3 were assigned a value of 2.0 g/cm^3, as previously described.[7] The ash density of each element, defined as a function of HU, was set as the average ash density of the voxels occupying the same volume in 3D space as the element. The Young modulus and yield stress for each element were assumed to be directionally isotropic and were calculated using published equations.[9]

Shell elements were assigned a Young modulus that matched the nearest tetrahedral element with an HU value of at least 600 HU. The Poisson ratio for each element was set at 0.3, as previously reported.[12] The Young modulus and Poisson ratio for the potting material were defined as 4.0 GPa and 0.4, respectively. An adhesive contact property between resin and bone was assigned.

Uniform displacement was applied to the potting material at the distal end of the radius at ramped displacement increments of 0.01 mm until the criteria for failure were met. The outer surfaces of the proximal potting material were encased. Each element was defined as yielding when its Druckere Prager equivalent stress reached the element yield stress. The fracture load was defined as the force at which a rapid decline in load was observed in the finite element analysis-predicted force displacement.[16]

Measurement of bone mineral density

The volumetric bone mineral density (vBMD) under the plate was measured using the quantitative CT evaluation of a 20-mm-long area of the forearm bone between the most distal proximal screw and the most distal plate screw (Fig. 3). The vBMD was also measured outside the plate. The vBMDs under and outside the plates of the affected and healthy sides were analyzed, and the ratio was calculated by dividing the vBMD of the affected side by that of the healthy side. This ratio was then evaluated over time.

Measurement of fracture load

The measurements of fracture load were conducted using the protocol from a previous validation study involving fresh-frozen cadavers.[15] On the healthy side, the fracture load of the same area was measured using CT/FEA. The fracture load was evaluated over time using the ratio of the fracture load of the affected side to that of the healthy side, which was calculated by dividing the value of the affected side by that of the healthy side.

Results

Postoperative imaging findings

The plain X-ray and CT images at various time points after the fixation of the ulnar fracture are presented in Figure 4A and B, respectively. Both imaging modalities revealed that the thinning of the radial and ulnar cortical bones just below the plate increased with time after surgery.

Postoperative bone mineral density

The vBMD under the plate of the ulna decreased with time after surgery (Fig. 4C). At 1 year after surgery, the vBMD under the plate of the radius and ulna of the healthy side was 92.3% and 84.6%, respectively (Fig. 5). The vBMD under the plate then remained

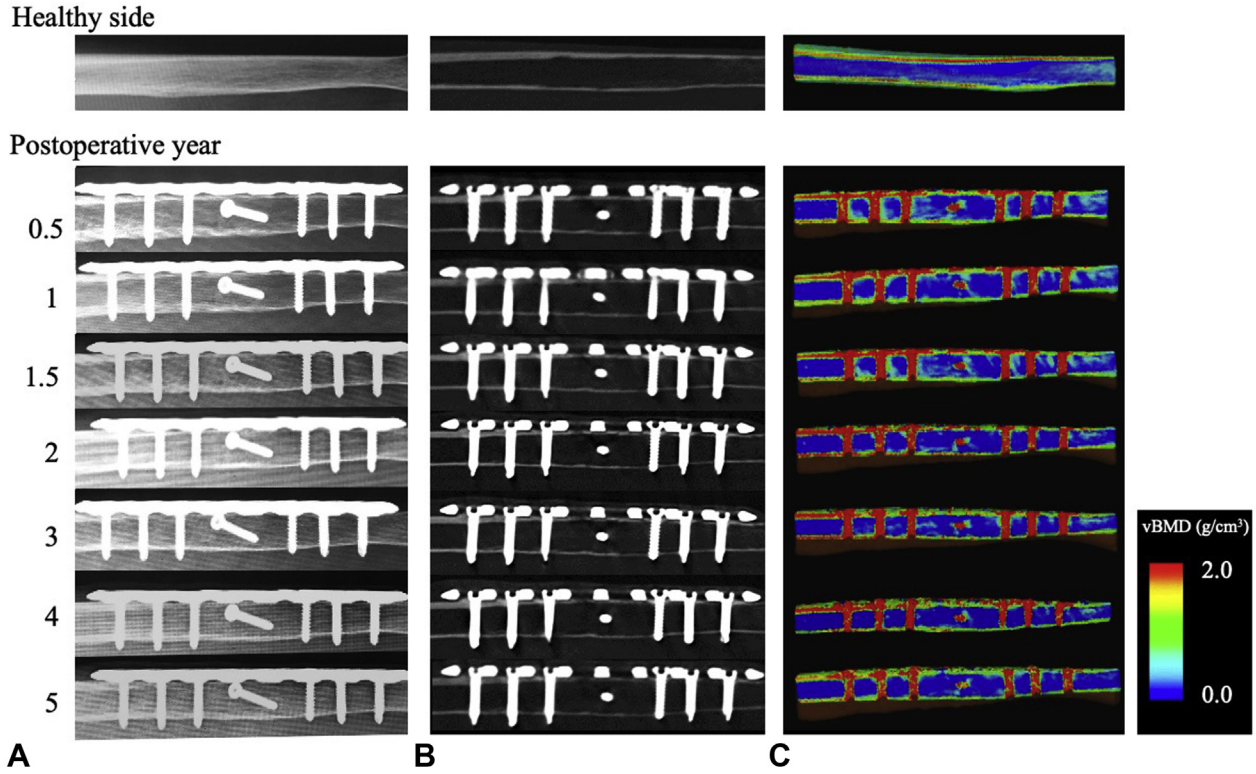

Figure 4. Postoperative imaging of the BMD of the ulna. **A** Plain X-ray images showing the thinning of the cortical bone just below the plate over time. **B** CT cross-sectional images revealing the thinning of the cortical bone just below the plate over the postoperative course. **C** BMD analysis of the central part of the plate showing decreased density over the postoperative course.

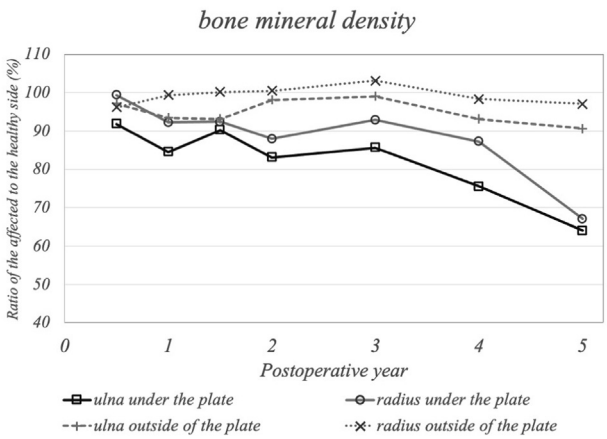

Figure 5. Graph of BMD at different time points after fixation. The BMD was stable between the first and third postoperative years but decreased markedly after the third postoperative year.

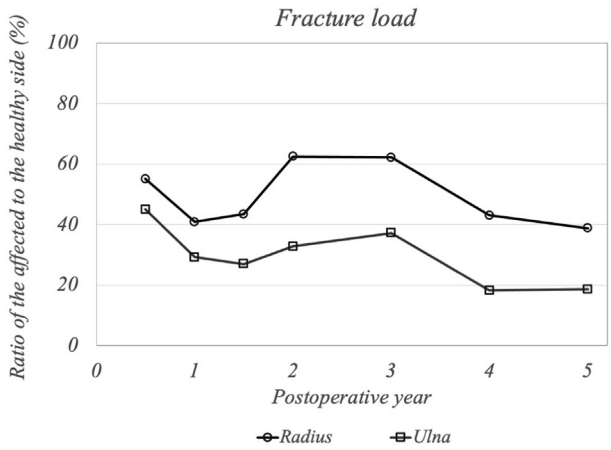

Figure 6. Graph of bone strength at different time points after fixation. Bone strength increased up until the third postoperative year, after which it began to decline.

almost unchanged until 3 years after surgery, after which a more pronounced decline was observed. At 5 years after surgery, the density of the radius and ulna of the healthy side was 67.1% and 64.0%, respectively. However, the vBMD outside the plate at each time point did not change.

Postoperative fracture load

At 1 year after surgery, the strength of the radius and ulna of the healthy side was 40.9% and 29.3%, respectively (Fig. 6). From the second to the third postoperative year, the fracture load of the radius and ulna of the healthy side increased to 62.2% and 37.3%, respectively; however, after the third year, the fracture load of the healthy side began to decline and reached 38.8% and 18.9% for the radius and ulna, respectively, at 5 years after surgery.

Discussion

This study demonstrated that the fracture load in the radius and ulna increased from the first to the third postoperative year, likely

because of remodeling during the healing process. However, the vBMD and bone strength decreased after the third postoperative year, although the bone density outside the plate did not change. Stress shielding and impaired circulation in the periosteum that is in contact with the plate have been reported to cause local bone atrophy after plate fixation.[5,17] Considering that the locking plate preserves periosteal blood flow because no crimping force is applied to the bone, the observed bone atrophy may have been due to stress shielding.[18,19] The prolonged loss of mechanical stimulation may have also decreased bone formation, resulting in a decreased bone mineral density (BMD) and fracture load.

Some discrepancies in the BMD and fracture load trends were observed in this study. We speculate that this is because the BMD represents an average of the regions, whereas the fracture load depends on the localization of BMD. Thus, an increased BMD and the resultant thickening of the cortical bone affect the strength rather than the cancellous BMD, which suggests that changes in BMD do not directly reflect changes in bone strength. The measurement of fracture load using CT or FEA should, therefore, be considered to assess bone strength.

The progressive bone atrophy suggests that plate stiffness is higher than the appropriate stiffness for bone creation because of the load on the forearm bones. A possible solution may be to approach the problem from the plate material side. We expect that biocompatible, low-stiffness alloys will be developed along with technology that disperses and reduces stress shielding by providing a stiffness gradient within the plate through the heat treatment of alloys and 3D-printing technology.

The present study has some limitations that should be acknowledged. First, this included a single case with only 2 forearms. A large number of cases should be evaluated in future investigations because of the variability that exists across cases. Further studies involving more cases are warranted to clarify the outcomes of long-term plate fixation. Second, FEA is only a simulation and does not necessarily reflect the fracture risk in clinical practice. Although our method of the measurement of fracture load was based on the static compression of axial pressure, external forces, such as bending, torsion, and shear, also exist, which can be complex and overlapping in actual fractures. Therefore, we believe that measuring fracture loads in response to different types of forces and comprehensively evaluating them can provide a more clinically relevant estimate of fracture risk. There is also the limitation that this patient had a fractured humerus. The reduced use of the upper extremity may have decreased the load on the forearm, resulting in bone atrophy. Lastly, the use of locking plate fixation for a forearm diaphyseal fracture would not necessarily be favored in a noncomminuted or nonosteoporotic bone; so, the applicability of the study results may be limited to specific clinical scenarios.

This study shows that open reduction and internal fixation of forearm diaphyseal fractures using a locking plate is associated with long-term, progressive bone atrophy. We believe that surgeons should be cognizant of the potential local bone atrophy that may result from the long-term fixation of locking plates and counsel their patients appropriately.

References

1. Hertel R, Pisan M, Lambert S, Ballmer FT. Plate osteosynthesis of diaphyseal fractures of the radius and ulna. *Injury*. 1996;27(8):545–548.
2. Leung F, Chow SP. Locking compression plate in the treatment of forearm fractures: a prospective study. *J Orthop Surg (Hong Kong)*. 2006;14(3):291–294.
3. Morisaki S, Hiraoka N, Fujiwara H, et al. Removal of plates from diaphyseal forearm fractures: comparison of dynamic compression plates and locking compression plates. *J Jpn Soc Fracture Repair*. 2018;40(4):1135–1139.
4. Ferguson SJ, UP Wyss, Pichora DR. Finite element stress analysis of a hybrid fracture fixation plate. *Med Eng Phys*. 1996;18(3):241–250.
5. Perren SM, Cordey J, Rahn BA, Gautier E, Schneider E. Early temporary porosis of bone induced by internal fixation implants. A reaction to necrosis, not to stress protection? *Clin Orthop Relat Res*. 1988;(232):139–151.
6. Klaue K, Fengels I, Perren SM. Long-term effects of plate osteosynthesis: comparison of four different plates. *Injury*. 2000;31(suppl 2):51–86.
7. Fulkerson E, Egol KA, Kubiak EN, Liporace F, Kummer FJ, Koval KJ. Fixation of diaphyseal fractures with a segmental defect: a biomechanical comparison of locked and conventional plating techniques. *J Trauma*. 2006;60(4):830–835.
8. Cordey J, Perren SM, Steinemann SG. Stress protection due to plates: myth or reality? A parametric analysis made using the composite beam theory. *Injury*. 2000;31(suppl 3):C1–C13.
9. Keyak JH. Improved prediction of proximal femoral fracture load using nonlinear finite element models. *Med Eng Phys*. 2001;23(3):165–173.
10. Imai K, Ohnishi I, Bessho M, Nakamura K. Nonlinear finite element model predicts vertebral bone strength and fracture site. *Spine*. 2006;31(16):1789–1794.
11. Matsuura Y, Kuniyoshi K, Suzuki T, et al. Accuracy of specimen-specific nonlinear finite element analysis for evaluation of distal radius strength in cadaver material. *J Orthop Sci*. 2014;19(6):1012–1018.
12. Arias-Moreno AJ, Hosseini HS, Bevers M, Ito K, Zysset P, van Rietbergen B. Validation of distal radius failure load predictions by homogenized- and micro-finite element analyses based on second-generation high-resolution peripheral quantitative CT images. *Osteoporos Int*. 2019;30(7):1433–1443.
13. Johnson JE, Troy KL. Validation of a new multiscale finite element analysis approach at the distal radius. *Med Eng Phys*. 2017;44:16–24.
14. Edwards WB, Troy KL. Finite element prediction of surface strain and fracture strength at the distal radius. *Med Eng Phys*. 2012;34(3):290–298.
15. Matsuura Y, Kuniyoshi K, Suzuki T, et al. Accuracy of specimen-specific nonlinear finite element analysis for evaluation of radial diaphysis strength in cadaver material. *Comput Methods Bionzech Biomed Engin*. 2015;18(16):1811–1817.
16. Matsuura Y, Kuniyoshi K, Takahashi K, et al. Bone atrophy after treatment of forearm fracture with locking plate using non-liner finite element analysis. *J Hand Surg Am*. 2017;42(8):659.
17. Tonino AJ, Davidson CL, Klopper PJ, et al. Protection from stress in bone and its effects. Experiments with stainless steel and plastic plates in dogs. *J Bone Joint Surg Br*. 1976;58(1):107–113.
18. Frigg R. Locking compression plate (LCP). An osteosynthesis plate based on the dynamic compression plate and point contact fixator (PC-Fix). *Injury*. 2001;32(suppl 2):63–66.
19. Takayama T, Uchikura C, Hirano J, et al. Histological evaluation of periosteum on Smith's fracture treated by LCP. *J Jpn Soc Fracture Repair*. 2005;27(1):324–326.